HNPS Advances in Nuclear Physics

Vol 31 (2025)

HNPS2024

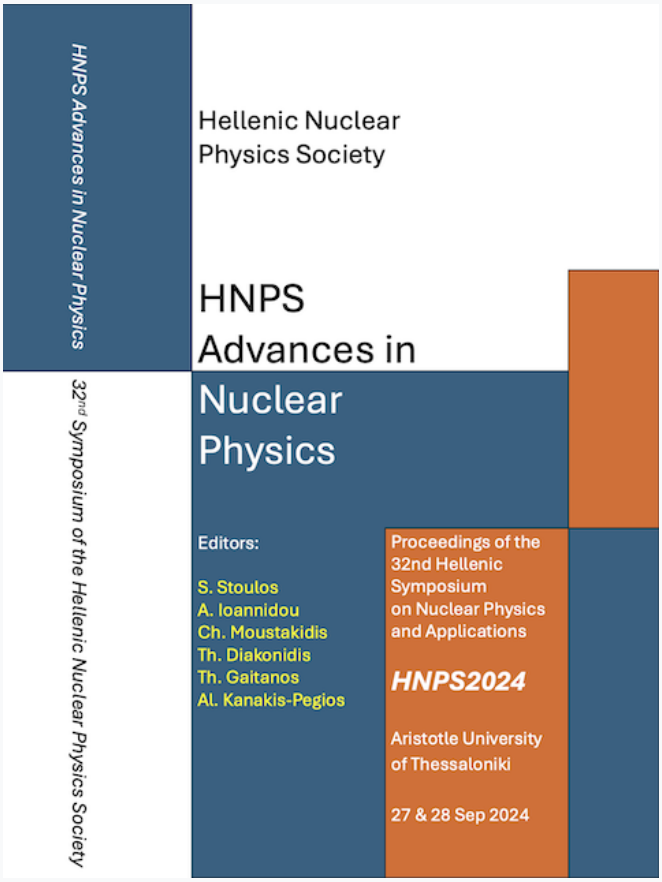


# Calibration of a whole-body counter system for dose assessment in emergency situations

*Konstantina Papadopoulou, Antonios Nikolakis-Plytzanopoulos, Nikolaos Salpadimos, Maria Kolovou, Konstantinos Karfopoulos, Constantinos Potiriadis*

doi: 10.12681/hnpsanp.7967



**To cite this article:**

Papadopoulou, K., Nikolakis-Plytzanopoulos, A., Salpadimos, N., Kolovou, M., Karfopoulos, K., & Potiriadis, C. (2025). Calibration of a whole-body counter system for dose assessment in emergency situations. *HNPS Advances in Nuclear Physics*, *31*, 41–47. https://doi.org/10.12681/hnpsanp.7967

# Calibration of a whole-body counter system for dose assessment in emergency situations

K. Papadopoulou[1,2,*], A. Nikolakis-Plytzanopoulos[1,2], N. Salpadimos[1], M. Kolovou[1], K. Karfopoulos[† 1], C. Potiriadis[1]

[1] *Environmental Radioactivity Monitoring Unit, Greek Atomic Energy Commission (EEAE)*
[2] *School of Medicine, National and Kapodistrian University of Athens, Athens, Greece*

**Abstract** Nuclear-propelled vessels (e.g. ships and submarines) are often stationed in the Greek port of Souda. To this end, a hypothetical release from a nuclear-powered submarine was produced and studied, using the decision-support system JRODOS. The study focused on determining the radiological risk to workers of the port. It was found that the internal contamination due to inhalation contributed more than 95% of the total effective dose, which was calculated as 175 mSv, assuming an 8-hour shift. Hence, the present study focused on internal dosimetry, by utilizing a Whole-Body Counter setup.

The Whole-Body Counter (WBC) setup of Greek Atomic Energy Commission was calibrated experimentally and via Monte Carlo (MC). The RMC-II phantom was used to calibrate the system experimentally. The Monte Carlo code PENELOPE was applied to model and calibrate the system. The MC efficiency calibration was within 6% mean relative bias compared to the experimental. The Minimum Detectable Activity (MDA) of the setup was calculated for every radionuclide considered from the hypothetical accident scenario, and detailed internal dose assessment was performed for the representative worker. The results were compared with the ones obtained by JRODOS.

**Keywords** Whole-body Counter, Internal dosimetry, Minimum detectable activity (MDA), Calibration, Monte-Carlo

## INTRODUCTION

The Greek Atomic Energy Commission (*EEAE*) is the national regulatory authority, competent for the control, regulation, and supervision in the fields of nuclear energy, nuclear technology, radiological and nuclear safety, and radiation protection. Within its mandate is to assess radiological and nuclear emergencies, which may entail radiological risk for the country [1]. In radiological emergency situations, rapid and accurate assessment of internal radiation exposure is critical to protect workers and the public. Whole-body Counters (WBCs) are essential tools for measuring radionuclide uptake and calculating internal doses. The Greek Atomic Energy Commission has implemented a dual-detector WBC system to enhance sensitivity and precision in such scenarios. This study aims to calibrate the EEAE's WBC system with hardware and Monte-Carlo techniques and to develop emergency dosimetric scenarios to guide occupational health measures.

The calibration process incorporates both experimental and Monte Carlo (MC) modeling approaches, leveraging the PENELOPE [2] software to simulate complex measurement scenarios. The PENELOPE model is further refined to address materials and detector-specific characteristics, contributing to robust emergency dose assessments. Additionally, this study benchmarks the Minimum Detectable Activity (MDA) [3] against international data to evaluate the WBC's reliability in emergency response applications.

* Corresponding author: kpapadopoyloy3499@gmail.com

## EXPERIMENTAL DETAILS

### *Experimental setup*

This study utilizes an ACCUSCAN shadow-shield scanning bed type whole-body Counter (WBC), equipped with a HPGe (GC2520) of 25% nominal efficiency and a NaI(Tl) detector, manufactured by Canberra (Fig. 1, *left*), installed in Greek Atomic Energy Commission (EEAE). The system is supported by the RMC-II calibration phantom and $^{137}$Cs, $^{60}$Co, $^{152}$Eu, $^{241}$Am sources are being utilized for calibration purposes. The RMC-II phantom is constructed by acrylic glass slabs with sockets that emulate a torso and neck region. The calibration sources can be placed in special sockets simulating the thyroid, lungs, total body and GI tract contamination (Fig. 1, *right*). The system collects data from the detectors either during whole-body scanning (moving bed measurement) or while the bed remains stationary. Measurement data are transmitted to a PC where they are processed with compatible software: Apex-In Vivo and Genie-2000 software.

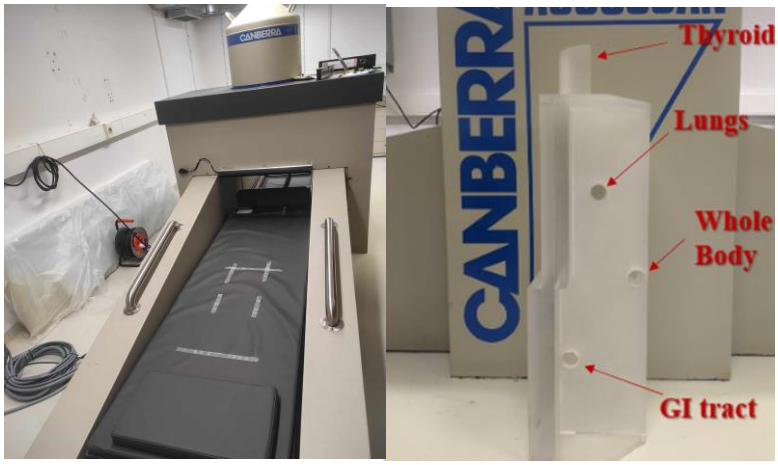


**Figure 1.** *(left) The Whole body Counter system of EEAE (right)The RMC-II phantom*

### *Calibration Operations*

Firstly, calibration operations take place using all the available sources. The energy calibration as well as the FWHM calibration are performed utilizing Apex-in Vivo's automatic calibration. Efficiency calibration is performed with each source placed in a different phantom socket at a time, for stationery and total body bed scans. Each measurement ends after collecting at least 10'000 counts per photopeak, to achieve the required uncertainty. The efficiency is then measured via the formula:

$$Eff = \frac{N}{A \cdot yield} \quad (1)$$

where *A* stands for the activity of the source, *N* for the net counts measured and (yield) corresponds to the photons/decay of each source. The efficiency curves $ln(Eff) = f(ln(E))$ for every setup are extracted and a 5$^{th}$ degree polynomial is fitted to the data (Figs. 2 & 3, see blue curves). For the Total Body scan, the $^{241}$Am source is not used as collecting enough counts was very time consuming due to the low energy and activity of the source.

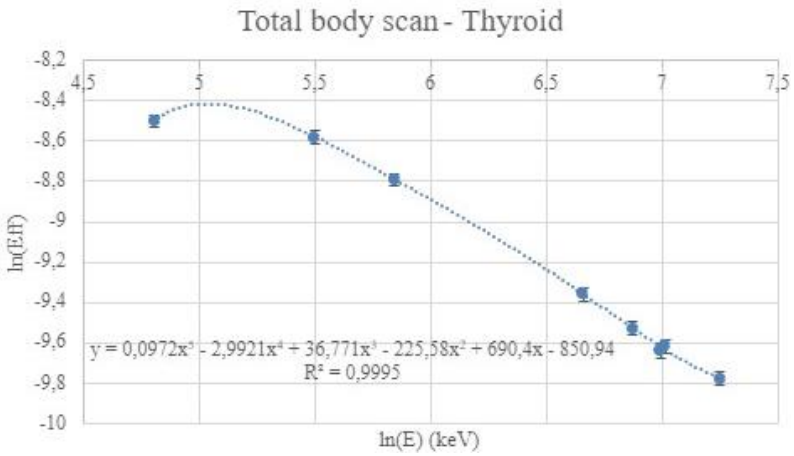


**Figure 2**. *Efficiency curve for total body scan in the thyroid region*

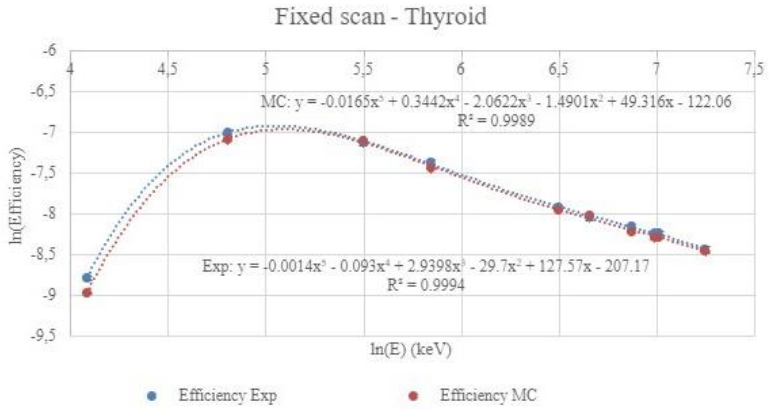


**Figure 3**. *Efficiency curve for fixed body scan in the thyroid region.*

*WBC modelling in PENELOPE*

The details provided by the manufacturing company and the bibliography regarding the internal dimensions of the HPGe detector, as well as the material of the WBC shielding, could benefit from further elaboration to ensure greater clarity. To overcome this challenge a similar detector (GC2020) with comparable properties is considered to model the HPGe detector of this study using typical values and proportion relations. The uncertainties of this assumption are integrated and co-evaluated in the detector's dead layers. Three distinct dead layers (frontward, lateral, and rear) are modeled, with thicknesses determined by iterative testing. Each layer's influence on sensitivity to specific photon energies is assessed using sources such as $^{241}$Am for the frontward layer, $^{137}$Cs for the lateral, and $^{60}$Co for the rear. For the determination of the thicknesses of the dead layers, it is necessary to take measurements that will serve as reference measurements for comparison with the computational results. The following algorithm is then applied:

1. The dead layer to be determined and the source to be simulated are selected.
2. A value for the thickness of the dead layer is defined in PENELOPE, and the simulation is executed using the same geometry as the reference measurements, until sufficient statistics are collected (Rel. Error < 5% (3σ)).
3. The computational efficiency of the detector for the specific dead layer thickness is estimated.
4. The computational efficiency is compared to the experimental efficiency using the relative bias criterion:

$$B_{rel} = \frac{\varepsilon_E^{exp} - \varepsilon_E^{MC}}{\varepsilon_E^{exp}} \cdot 100\% \quad (2)$$

where $\varepsilon_E^{exp}$ is the experimental efficiency calculated from the reference measurements, and $\varepsilon_E^{MC}$ is the computational efficiency calculated from the simulation results.

5. Steps 2–4 are repeated until the absolute value of equation (2) falls below 5%.

The final thicknesses of the dead layers were found to be: 2 mm for the frontward, 1.7 mm for the lateral and 2 mm for the rear one (Fig. 4). According to literature these dead layers are compatible with those of similar detectors e.g. Clouvas, et al. [4]. These thicknesses are cross-validated against measurements with $^{152}$Eu, achieving a mean relative bias of 4%, indicating good accuracy in the MC model (Table 1). Each source's activity has an uncertainty of 3%.

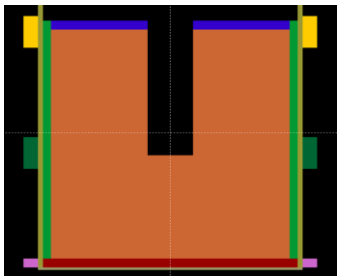

**Figure 4:** *The detector model in PENELOPE. With red the frontward, with green the lateral and with blue the rear dead layers as measured.*

**Table 1**. *Relative Bias of the experimental and simulated efficiencies measured with the final dead layer thicknesses of the HPGe GC2520 detector.*

| Isotope | Energy (keV) | $\varepsilon^{MC}$ | $\varepsilon^{exp}$ | Rel. Bias |
|---|---|---|---|---|
| $^{241}$Am | 59.5 | 1.73E-03 | 1.68E-03 | 3% |
| $^{137}$Cs | 661.7 | 2.69E-03 | 2.63E-03 | 2% |
| $^{60}$Co | 1173.2 | 1.61E-03 | 1.67E-03 | -4% |
| | 1332.5 | 1.46E-03 | 1.51E-03 | -4% |
| $^{152}$Eu | 121.8 | 8.43E-03 | 8.08E-03 | -4% |
| | 244.7 | 6.87E-03 | 6.19E-03 | -11% |
| | 344.3 | 4.87E-03 | 4.66E-03 | -5% |
| | 778.9 | 2.37E-03 | 2.27E-03 | -5% |
| | 964.1 | 1.97E-03 | 1.92E-03 | -3% |
| | 1085.8 | 1.79E-03 | 1.75E-03 | -2% |
| | 1112.1 | 1.75E-03 | 1.74E-03 | -1% |
| | 1408.0 | 1.44E-03 | 1.40E-03 | -2% |

To properly model the detector, its shielding was also considered. The shielding material composition is analyzed using X-Ray Fluorescence (XRF) with a SiPIN detector and a $^{241}$Am source. The analysis identifies iron (Fe) as the dominant material, with traces of chromium (Cr) and nickel (Ni). The MC model is set to use Fe as the primary shielding material for the simulation procedure.

The final model is then cross checked with the corresponding source measurements for fixed WBC scan. As seen in Fig. 3 through the red curve that represents the simulation data, the HPGe detector's response shows good convergence with experimental data (blue curve) for medium and high energies. However, deviations appear for low-energy photons, specifically near the 60 keV of $^{241}$Am. These differences, which have a relative bias between 15% and 30%, can be attributed to the approximations made during the development of the MC model. This limitation is considered non-critical as WBC systems are predominantly used for higher-energy detection, where photon attenuation is less impactful.

## RESULTS AND DISCUSSION

The calibration of the WBC system demonstrates robust performance across the range of medium-to-high photon energies, with certain limitations observed at lower energy levels. The key findings from the calibration process and emergency dosimetry scenarios are outlined below.

The Minimum Detectable Activity (MDA) for a standard acquisition time of 1200 s was calculated using the Curie methodology [3] for various γ-emitters placed in the whole-body socket of the phantom, as to measure the MDAs for the furthest position on the sources from the detector (worst case scenario). Additional information regarding the MDA methodology can be found in [5] and [6]. The MDA findings for $^{40}$K, $^{60}$Co, $^{131}$I, $^{134}$Cs and $^{137}$Cs are shown in Fig. 5. The isotope energies used in the calculation correspond to those with the highest yields, as they are more effectively detected by the system. The calculated MDA values for key isotopes (137-Cs: 402 Bq; 60-Co: 432 Bq) are in line with EURADOS 2004 levels [7], suggesting that the system's sensitivity meets international standards for emergency preparedness. In order to investigate the impact of co-contaminant sources in MDA assessment, the MDAs are also calculated with 60-Co and 137-Cs co-contaminant sources of activities 6.33 kBq and 28.7 kBq respectively in the thyroid region, as to create the biggest noise (worst case scenario), because that socket is closer to the detector, assuming whole-body contamination with the other isotopes. The results are shown in Figure 5.

Dosimetric scenarios for emergency situations were also produced and studied. The goal was to evaluate potential occupational exposure for respiration of radionuclides under emergency conditions. The model considers a slight variation from a practice of RODOS User Group [8] but this time there is a collision of a nuclear submarine and a freight ship, 2 km from Souda port in Greece. The result of the collision is the release of nuclear material in the air as those described in [9]. The concentration in air of various radionuclides released from the collision summed for 8 hours can be seen in table 2. To study the worst case scenario, the wind is considered to head towards the port, where a worker is on an 8h shift a) performing "light work" with a respiration rate of 1.5 $\frac{m^3}{h}$ [10] and b) performing "sitting" work with a respiration rate of 0.54 $\frac{m^3}{h}$ [10]. As such the two scenarios are modeled to simulate internal dose assessments, incorporating respiratory activity and environmental contamination levels. The JRODOS system, a sophisticated decision-support tool for radiological emergencies, is utilized to simulate and refine these dosimetric scenarios [11]. JRODOS allows for real-time assessment of radiological impacts, offering projections of airborne contamination spread and dose distribution that support scenario modeling and safety planning.

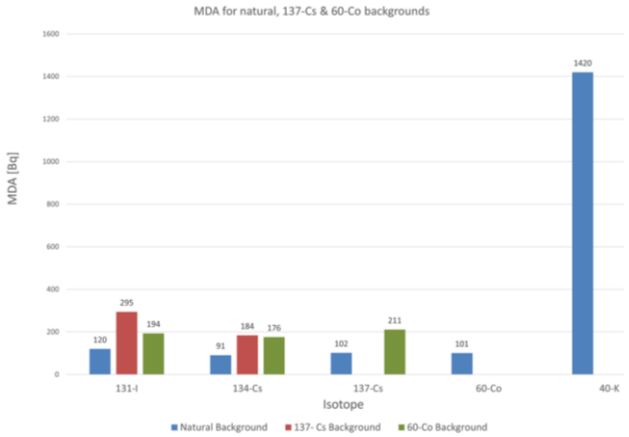


**Figure 5.** *The MDAs as measured for the different isotopes of interest and different background spectra: Blue color refers to measurements taken with natural background, red refers to $^{137}$Cs co-contaminant and green to $^{60}$Co co-contaminant.*

- **Light Work Scenario:** The effective dose due to inhalation is calculated using ICRP103 $w_T$ values to be 150 mSv for the whole 8h shift, based on intake estimates from airborne contamination of key radionuclides such as $^{137}$Cs, $^{134}$Cs, $^{133}$I, $^{135}$I and particularly $^{131}$I, which poses a significant thyroid dose risk and also has the biggest concentration in air (Table 2) and thus the biggest contribution to the effective dose. The projected effective dose in this scenario exceeds the IAEA's emergency dose threshold of 100 mSv, indicating a need for immediate protective actions. Recommended protective measures include limiting exposure duration, administering iodine tablets to block thyroid uptake, and ensuring that emergency protocols, such as alarms and limiting working time are established. In reality, safety measures would have been taken quickly and the workers' time spent at the port would have been limited, but this scenario demonstrates the importance of having emergency plans for possible nuclear accidents.
- **Sitting Scenario:** JRODOS simulations indicate that the calculated effective dose of 53 mSv from inhalation calculated using ICP103 $w_T$ values, remains below the IAEA emergency threshold. In this scenario, standard radiation protection protocols would be sufficient. Routine precautions such as limiting time in contaminated areas and adhering to respiratory protection guidelines, would adequately safeguard workers in a sedentary context.

**Table 2**. *Air concentration of various radionuclides near the ground summed for 8 hours.*

| Radioisotope | Air concentration for 8 h (MBq/m$^3$) |
|---|---|
| Cs-137 | 0.83 |
| Cs-134 | 0.67 |
| I-131 | 8.27 |
| I-133 | 0.04 |
| I-135 | 0.31 |

Internal contamination due to inhalation contributes more than 95% of the total effective dose, which is calculated by JRODOS to be 175 mSv, assuming an 8-hour light-work shift. Someone might reasonably wonder where the difference between the 148 mSv mentioned above and the 175 mSv mentioned here comes from. The difference between 148 and 175 mSv lies in the fact that the 148 mSv are calculated without considering all the released radionuclides. Since the MDAs are below 1 kBq and the released activities from the hypothetical accident are in the MBq or GBq area, the WBC of EEAE can be of service, even after a few days from the day of the accident. Thus, internal dosimetry via a WBC is an appropriate method of dose assessment.

## CONCLUSIONS

In this study the EEAE's WBC system is being calibrated successfully using both experimental and MC simulation methods. The virtual calibration approach via the PENELOPE software yields accurate efficiencies for medium-to-high photon energies, thus proving as a reliable method for calibrating a WBC system. The WBC's MDAs are validated against EURADOS benchmarks, confirming that the system's sensitivity aligns with international standards.

In the studied scenario involving light physical activity, the estimated occupational effective dose exceeds the 100 mSv emergency threshold, indicating the need for immediate protective actions, such as restricted exposure times and iodine prophylaxis. Conversely, sedentary activities result in lower dose estimates, suggesting that standard radiation protection practices would suffice.

## References

[1] European Council Directive 2013/59/Euratom on basic safety standards for protection against the dangers arising from exposure to ionising radiation and repealing Directives 89/618/Euratom, 90/641/Euratom, 96/29/Euratom, 97/43/Euratom and 2003/122/Euratom. OJ of the EU. L13; 57: 1–73 (2014).
[2] NEA (2019), PENELOPE 2018: A code system for Monte Carlo simulation of electron and photon transport: Workshop Proceedings, Barcelona, Spain, 28 January – 1 February 2019, OECD Publishing, Paris; doi: 10.1787/32da5043-en.
[3] D.J. Strom, et al., Health Phys. 63, 360 (1992)
[4] A. Clouvas, et al., Health Phys. 74, 216 (1998)
[5] A. Nikolakis-Plytzanopoulos. “Utilization of a whole-body counter system for internal dosimetry due to planned exposure”, url: https://pergamos.lib.uoa.gr/uoa/dl/object/3398818
[6] K. Papadopoulou, “Internal dosimetry methods in emergency situations”, url: https://pergamos.lib.uoa.gr/uoa/dl/object/3398782
[7] M.A. Lopez Ponte, et al., Rad. Prot. Dosim. 112, 69 (2004); doi: 10.1093/rpd/nch284
[8] P.L. Ølgaard, et al., Nordic nuclear safety research-NKS-139, April 2006.
[9] H. Eikelmann, et al., Nordic nuclear safety research- NKS-390, May 2017.
[10] F. Paquet, et al., Annals of the ICRP 44, 5 (2015); doi: 10.1177/0146645315577539.
[11] W. Raskob, et al., Radioprot. 46, S731 (2012); doi: 10.1051/radiopro/20116865s.